

- (15) Pikal, M. J., Spedding, F. H., USAEC Rept., IS-1344, 1968.
 (16) Redlich, O., Meyer, D., *Chem. Rev.*, **64**, 221 (1964).
 (17) Spedding, F. H., Cullen, P. F., Habenschuss, A., *J. Phys. Chem.*, **78**, 1106 (1974).
 (18) Spedding, F. H., Pikal, M. J., Ayers, B. O., *ibid.*, **70**, 2440 (1966).
 (19) Spedding, F. H., Rard, J. A., *ibid.*, **78**, 1435 (1974).
 (20) Spedding, F. H., Saeger, V. W., Gray, K. A., Boneau, P. K., Brown, M. A., DeKock, C. W., Baker, J. L., Shiers, L. E., Weber, H. O., Habenschuss, A., *J. Chem. Eng. Data*, **20** (1), 72 (1975).
 (21) Spedding, F. H., Shiers, L. E., Rard, J. A., *ibid.*, p 66.
 (22) Sutcliffe, L. H., Weber, J. R., *Trans. Faraday Soc.*, **52**, 2225 (1956).
 (23) Sutton, J., *Nature*, **169**, 71 (1952).
 (24) Templeton, D. H., Dauben, C. H., *J. Amer. Chem. Soc.*, **76**, 5237 (1954).
 (25) Tilton, L. W., Taylor, J. K., *J. Res. Nat. Bur. Stand.*, **18**, 205 (1937).

Received for review June 21, 1974. Accepted October 4, 1974.

Relative Viscosities of Some Aqueous Rare Earth Nitrate Solutions at 25°C

Frank H. Spedding,¹ Loren E. Shiers, and Joseph A. Rard

Ames Laboratory-USAEC and Department of Chemistry, Iowa State University, Ames, Iowa 50010

The relative viscosities of aqueous solutions of the trivalent nitrates of La, Pr, Nd, Sm, Gd, Tb, Dy, Ho, Er, Yb, and Lu were measured over the concentration range of approximately 0.05*m* to saturation at 25°C. The relative viscosities of the aqueous rare earth chlorides and perchlorates were reported previously. The rare earth nitrate relative viscosities at constant molal concentrations increased regularly from La to Lu. The nitrate viscosity data are briefly compared to the chloride and perchlorate viscosities, and the trends in the nitrate viscosities are briefly discussed in terms of complexation between the rare earth and nitrate ions and in terms of hydration changes across the rare earth series.

In dilute rare earth nitrate solutions it is believed that a mixture of inner and outer sphere complexation occurs between the rare earth and nitrate ions (2, 3) with the major species being outer sphere. In more concentrated solutions the predominant form of interaction appears to be inner sphere with binding probably occurring through the oxygens of the nitrates (1, 4, 5, 8, 10). In addition, three nitrates are doubly coordinated to the rare earth ion in the hydrated crystals (11).

The trends observed in the rare earth chloride and perchlorate transport properties (13, 15, 16, 18, 19) are consistent with a change in the inner sphere hydration of the rare earth ion and with changes in overall hydration across the rare earth series. The formation of inner sphere complexes in the rare earth nitrates would result in the displacement of inner sphere water; consequently, the same explanation will not be expected to hold for the rare earth nitrates except in very dilute solutions. This study was undertaken to investigate the effect of inner sphere complexation on rare earth salt solution transport properties.

Experimental

The viscosities were measured at 25°C with the same suspended level Ubbelohde viscometers that were used for the rare earth chloride (13, 19) and perchlorate (18) viscosity determinations. The experimental techniques and procedures were the same as previously reported (13). Stock solutions of the stoichiometric salts were prepared by the method of Spedding et al. (14), and dilu-

tions were prepared by weight from conductivity water and stock solution. All stock and saturated solutions were analyzed by EDTA (12) and sulfate (14) methods; these analyses agreed to ±0.1% or better in terms of the molality. In performing the sulfate analyses, the nitrate ions were decomposed by evaporating the samples with hydrochloric acid before the sulfuric acid additions were made.

Errors and Data Treatment

The kinetic energy corrections are negligible for the viscometers used in this research; therefore, the relative viscosities are given by

$$\eta_R = dt/d_0t_0 \quad (1)$$

where d is the solution density, d_0 the water density, t the solution efflux time, and t_0 the water efflux time. The densities of the solutions studied in this research will be reported separately along with the partial molal volumes (17). In Table I the experimental relative viscosities and the corresponding molal concentrations of the solutions are listed. Except for Pr(NO₃)₃, the highest concentration in each case is the saturated solution. The highest concentration for Pr(NO₃)₃ is a supersaturated solution.

The errors in the solution densities are negligible compared to the other experimental errors. The total error in each viscosity is then mainly due to the error in the viscosity measurement and to the solution concentration uncertainty. The solution concentration uncertainties are ±0.1% or less, and the experimental viscosity determinations are reliable to at least ±0.05%. The total maximum probable error in the viscosity, when the concentration uncertainty is included, is 0.13% at 1.0*m*, 0.23% at 2.0*m*, 0.32% at 3.0*m*, 0.40% at 4.0*m*, 0.47% at 5.0*m*, 0.54% at 6.0*m*, and 0.78% at 6.8*m*. The relative concentration uncertainties for each salt are much smaller than the above numbers since the dilutions were prepared by weight from a concentrated stock solution and conductivity water. Since the measured viscosity data for each salt, except for the saturated solution, are self-consistent to within 0.05%, the data in Table I are given to five figures.

The rare earth nitrate viscosity data were fitted to the equation

$$\frac{\eta_R - 1}{\eta_R} = \sum_{i=1}^6 A_i m^{i/2} \quad (2)$$

¹ To whom correspondence should be addressed.

Table I. Experimental Relative Viscosities at 25°C

<i>m</i>	η_R	$\Delta, \%$	<i>m</i>	η_R	$\Delta, \%$
La(NO₃)₃			Sm(NO₃)₃		
0.041384	1.0243	+0.14	0.01026	1.0106	+0.03
0.076359	1.0416	+0.07	0.02229	1.0172	+0.07
0.093896	1.0508	-0.02	0.05009	1.0316	+0.06
0.15991	1.0846	-0.14	0.07826	1.0466	-0.03
0.24983	1.1320	-0.14	0.10059	1.0574	-0.01
0.35981	1.1942	-0.07	0.25117	1.1402	-0.18
0.48912	1.2740	+0.05	0.49468	1.2926	-0.08
0.63972	1.3778	+0.15	0.75200	1.4854	+0.17
1.0003	1.6812	+0.14	1.0107	1.7233	-0.23
1.3323	2.0388	+0.11	1.2834	2.0286	+0.08
1.6345	2.4509	-0.08	1.5943	2.4598	-0.04
1.9598	3.0050	-0.15	1.8961	2.9812	-0.09
2.0915	3.2684	-0.13	2.1973	3.6274	-0.03
2.5231	4.3280	+0.15	2.4808	4.3856	-0.07
2.8925	5.5322 ^a	(+0.79)	2.8069	5.4764	-0.02
3.2133	6.9856	-0.03	3.1028	6.7284	-0.05
3.6055	9.2632	+0.05	3.3953	8.2592	+0.09
3.9997	12.436	-0.05	3.7033	10.312	-0.02
4.4561	17.716	+0.03	4.1149	13.985	-0.14
4.6100	20.078	-0.01	4.2811	15.833	+0.15
Pr(NO₃)₃			Gd(NO₃)₃		
0.012761	1.0094	+0.23	0.099982	1.0591	+0.08
0.020024	1.0159	-0.03	0.15663	1.0904	-0.02
0.044787	1.0262	+0.14	0.25001	1.1439	-0.08
0.084666	1.0464	-0.01	0.35970	1.2114	-0.08
0.10226	1.0555	-0.09	0.49084	1.2994	-0.04
0.25606	1.1365	-0.23	0.64170	1.4112	+0.06
0.50826	1.2909	-0.10	0.81139	1.5534	+0.12
0.77666	1.4908	+0.07	1.0044	1.7402	+0.09
1.0259	1.7149	+0.22	1.2106	1.9708	+0.05
1.3353	2.0585	+0.18	1.4396	2.2740	-0.14
1.6482	2.4948	+0.04	1.6917	2.6631	+0.02
1.9796	3.0738	+0.04	1.9667	3.1847	-0.05
2.2873	3.7564	-0.06	2.2544	3.8561	-0.03
2.6134	4.6684	-0.08	2.5658	4.7646	-0.04
2.9405	5.8371	-0.06	2.8961	5.9819	+0.08
3.2453	7.2244	-0.02	3.2383	7.6151	+0.06
3.5734	9.1354	+0.06	3.6224	10.057	-0.16
3.9246	11.834	+0.07	3.9515	12.788	+0.11
4.2189	14.797	+0.01	4.3766	17.850	-0.03
4.5344	18.943	-0.10			
4.9102	25.682	-0.09			
5.2340 ^b	33.738	+0.15			
Nd(NO₃)₃			Tb(NO₃)₃		
0.010038	1.0076	+0.16	0.008601	1.0085	+0.12
0.030079	1.0188	+0.08	0.016848	1.0142	+0.09
0.050770	1.0295	+0.01	0.034537	1.0251	+0.03
0.099610	1.0540	-0.09	0.094733	1.0589	-0.06
0.24481	1.1307	-0.19	0.15741	1.0938	-0.05
0.54592	1.3181	+0.01	0.23503	1.1396	-0.07
0.69958	1.4319	+0.08	0.35715	1.2166	-0.05
0.87432	1.5786	+0.11	0.46609	1.2923	-0.09
1.0862	1.7834	+0.11	0.67485	1.4515	+0.10
1.5994	2.4302	+0.08	0.86019	1.6160	+0.16
1.8489	2.8462	-0.05	1.0453	1.8068	+0.04
2.1272	3.4055	-0.07	1.2095	1.9962	+0.08
2.4525	4.2265	-0.15	1.5350	2.4480	+0.03
2.8288	5.4506	+0.01	1.7525	2.8176	-0.06
3.2481	7.3036	+0.08	2.0198	3.3570	-0.05
3.7528	10.522	-0.05	2.3845	4.2858	+0.01
4.4850	18.363	-0.04	2.7500	5.5153	+0.10
4.6184	20.440	+0.06	3.1932	7.4768 ^a	(+0.46)
			3.6250	10.188	+0.15
			3.9249	12.673	-0.09
			4.3234	17.036	-0.09
			4.5395	20.152	+0.11

(Continued on page 90)

Table I. Continued

<i>m</i>	η_R	$\Delta, \%$	<i>m</i>	η_R	$\Delta, \%$
	Dy(NO ₃) ₃			Er(NO ₃) ₃	
0.02582	1.0210	+0.09	3.9871	13.956	+0.01
0.05171	1.0358	+0.06	4.3986	18.830	0.00
0.08631	1.0553	0.00	4.9790	29.278	-0.10
0.12316	1.0769	-0.11	5.1718	33.995	-0.15
0.20836	1.1267	-0.15	5.4348	41.240	+0.32
0.40587	1.2548	-0.10		Yb(NO ₃) ₃	
0.65455	1.4454	+0.02	0.010910	1.0108	+0.26
0.89451	1.6657	+0.13	0.039933	1.0288	+0.15
1.2055	2.0172	+0.10	0.089004	1.0562	+0.04
1.4951	2.4239	+0.06	0.15961	1.0987	-0.21
1.7927	2.9425	-0.06	0.26098	1.1622	-0.26
2.0997	3.6051	-0.07	0.49754	1.3336	-0.11
2.3790	4.3506	-0.08	0.68938	1.5006	+0.01
2.6907	5.3782	0.00	0.83623	1.6474	+0.08
2.9627	6.4880	+0.03	1.0147	1.8475	+0.32
3.2857	8.1326	+0.02	1.2110	2.1091	+0.22
3.5855	10.056	+0.01	1.4608	2.5030	+0.15
3.8724	12.362	-0.02	1.6868	2.9348	-0.07
4.1729	15.416	-0.01	1.9627	3.5664	-0.15
4.7382	24.008	+0.01	2.2492	4.3770	+0.25
	Ho(NO ₃) ₃		2.5522	5.4316	+0.03
0.015019	1.0084	+0.35	2.8990	6.9577	-0.05
0.048979	1.0290	+0.08	3.2261	8.7912	-0.02
0.080570	1.0470	-0.06	3.5764	11.274	+0.13
0.10262	1.0599	-0.15	3.9936	15.212	+0.01
0.25260	1.1495	-0.26	4.4452	21.136	-0.15
0.51386	1.3316	-0.04	4.8152	27.788	+0.03
0.74507	1.5260	+0.19	5.3065	40.394	+0.04
1.0038	1.7886	+0.31	5.7613	57.826	-0.17 ^c
1.2960	2.1556	+0.16	6.2791	87.328	+0.29 ^c
1.8958	3.1968	-0.03	6.6500	124.32 ^a
2.2048	3.9418	-0.29		Lu(NO ₃) ₃	
2.5060	4.8250	-0.08	0.021459	1.0178	+0.24
2.7897	5.8557	-0.01	0.052078	1.0354	+0.14
3.1053	7.2782	+0.09	0.078303	1.0506	+0.01
3.4038	8.9718	+0.05	0.10185	1.0642	-0.08
3.7089	11.142	0.00	0.12013	1.0758	-0.22
4.0116	13.860	-0.03	0.25639	1.1615 ^a	(-0.51)
4.3767	18.166	-0.17	0.48636	1.3265	-0.22
4.5945	21.370	+0.06	0.70229	1.5158	+0.01
4.8080	25.155	+0.21	1.0174	1.8612	+0.25
5.0184	29.773	-0.15	1.2251	2.1432	+0.28
	Er(NO ₃) ₃		1.5888	2.7693	+0.07
0.0084509	1.0072	+0.26	1.9073	3.4811	-0.05
0.018296	1.0139	+0.18	2.1106	4.0316	-0.04
0.052290	1.0344	-0.07	2.4492	5.1632	-0.13
0.077123	1.0490	-0.23	2.7150	6.2648	-0.07
0.094973	1.0541	+0.18	3.0163	7.7952	+0.04
0.25759	1.1536	-0.21	3.4854	10.942	+0.11
0.51021	1.3342	-0.17	3.7220	12.986	+0.03
0.78850	1.5778	+0.10	4.0163	16.063	-0.03
1.0604	1.8733	+0.20	4.5152	23.110	-0.10
1.3576	2.2754	+0.14	5.0094	33.400	+0.07
1.6795	2.8194	+0.14	5.6401	54.541	0.00 ^c
2.0131	3.5345	+0.11	6.3225	96.126	-0.33 ^c
2.3210	4.3795	-0.27	6.8219	149.92	+0.25 ^c
2.6532	5.5018	-0.03			
2.9771	6.8759	-0.10			
3.3041	8.5776 ^a	(+0.52)			
3.6440	10.927	+0.12			

^a This point given a weight of zero. ^b Supersaturated solution. ^c Calculated from Equation 3.

Table II. Parameters for Viscosity Polynomial

Salt	A ₁ × 10	A ₂ × 10	A ₃	A ₄	A ₅ × 10	A ₆ × 10 ²
La(NO ₃) ₃	0.7886015	1.152401	0.6119364	-0.5452006	1.611693	-1.607515
Pr(NO ₃) ₃	0.8833258	0.5074379	0.7547986	-0.6712306	2.096805	-2.293623
Nd(NO ₃) ₃	0.7240428	1.312015	0.6200771	-0.5650215	1.695759	-1.711709
Sm(NO ₃) ₃	0.8933233	1.085414	0.6371495	-0.5694042	1.677218	-1.632337
Gd(NO ₃) ₃	0.9431371	1.232614	0.6186698	-0.5614688	1.654995	-1.591912
Tb(NO ₃) ₃	0.7944137	2.125430	0.4985254	-0.4911636	1.459862	-1.382776
Dy(NO ₃) ₃	0.9896777	1.169677	0.7016578	-0.6741236	2.186360	-2.442449
Ho(NO ₃) ₃	0.6654966	1.601520	0.7434797	-0.7578669	2.600177	-3.107851
Er(NO ₃) ₃	0.9468622	0.3252619	0.9672597	-0.9280485	3.182108	-3.847677
Yb(NO ₃) ₃ ^a	1.204638	-0.4613899	1.092697	-1.014609	3.439980	-4.121200
Lu(NO ₃) ₃ ^b	1.263484	-0.8878591	1.179524	-1.081770	3.663598	-4.393677

^a Applies to 5.3065*m*. ^b Applies to 5.0094*m*.

using the inverse square of the probable error as the statistical weight for each point. In this equation *m* is the molality. These coefficients are listed in Table II. In Table I the percent differences between the calculated and experimental viscosities are given. Above 1.2*m* these polynomials represent the viscosity data well within experimental error, whereas below this concentration systematic differences occur. Even in the dilute region the fits are not particularly bad, being within 0.3% of the experimental values in all cases, but the differences are outside the experimental errors.

Because of the large solubilities of Yb(NO₃)₃ and Lu(NO₃)₃, Equation 2 was not able to represent their viscosities up to saturation, and the fits were truncated at 5.3065*m* for Yb(NO₃)₃ and 5.0094*m* for Lu(NO₃)₃. The data for these two salts above 3.0*m* were then fitted to the equation

$$\frac{\eta_R - 1}{\eta_R} = \sum_{i=1}^4 B_i m^{i/4} \quad (3)$$

In the region of overlap, Equations 2 and 3 both accurately represent the data. These coefficients are listed in Table III. In the case of Yb(NO₃)₃, the saturated solution viscosity was not included in the fit. Since the stock and saturated solutions were analyzed separately, they can differ by as much as 0.7% from the correct viscosity. There could therefore be a maximum discrepancy of 1.4% in the viscosity between the stock and saturated solutions. Only in the case of Yb(NO₃)₃ was the actual discrepancy large enough to warrant dropping the saturated solution value.

Results

In Figure 1 the relative viscosities of the chloride (19), perchlorate (18), and nitrate of Lu are compared as a function of the molality. These curves are typical for the rare earths. In all cases, for any given rare earth, the chloride viscosity is highest, and the nitrate lowest at constant molality except at low concentrations where the nitrate viscosity falls between the chloride and perchlorate. Because of their solubilities, however, the heavy rare earth nitrates eventually become the most viscous, reaching a relative viscosity of 150 times that of water in the case of Lu(NO₃)₃.

In Figure 2 the percent differences between the viscosities calculated from Equation 2 and the experimental viscosities are shown for three of the salts studied. Equation 2 accurately represents the viscosity data at high concentrations, but the calculated values differ systematically from the experimental values at lower concentrations.

The full accuracy of the viscosity data cannot be seen on a direct plot of the size allowed here. Consequently, to present the data graphically so that real differences between the rare earth nitrates will appear, the ratios of the viscosities of interest to those of Lu(NO₃)₃

$$R = \eta_R^{RE(NO_3)_3} / \eta_R^{Lu(NO_3)_3} \quad (4)$$

were calculated as a function of the molality, and these ratios are shown in Figure 3. The apparent crossings at high concentrations may not be real since they occur between the stock and saturated solution values of one salt of each crossing pair of salts. In the case of the rare

Table III. Parameters for Equation 3

Salt	B ₁	B ₂	B ₃	B ₄
Yb(NO ₃) ₃	-6.889715	13.39754	-7.588015	1.433064
Lu(NO ₃) ₃	-7.316637	14.35274	-8.283045	1.598711

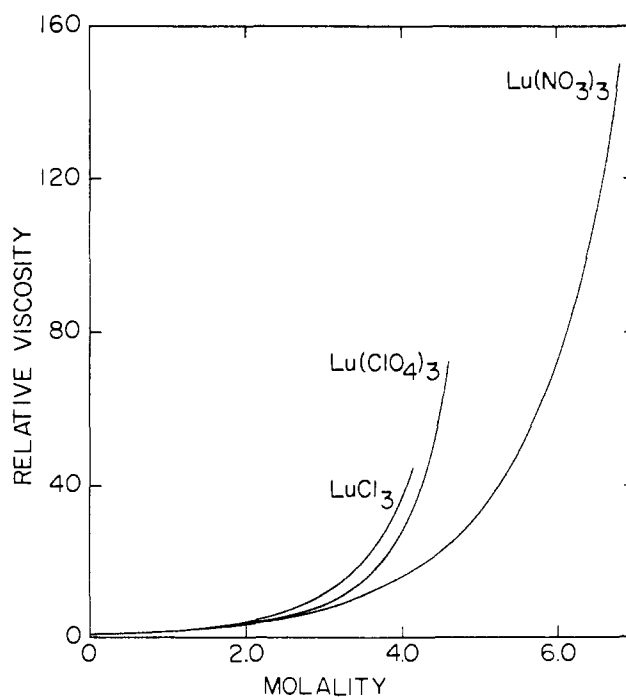


Figure 1. Relative viscosities of aqueous Lu electrolytes at 25°C as function of molality

earth chlorides (13, 19) and perchlorates (18), the ratios were calculated relative to lanthanum. Because of the larger variation in solubility for the rare earth nitrates, lutetium was chosen for reference purposes.

In Figures 4 and 5 constant molal plots of these ratios are given for the nitrates as a function of the ionic radius

(20). At 1.0*m* the viscosity rises slowly from La to Nd and then increases more rapidly to Lu. At this concentration the corresponding curves for the chlorides and perchlorates show a pronounced S shape which is absent in the nitrates. The Jones-Dole *B*-coefficients also exhibit an S shape in the chlorides and perchlorates. Note that

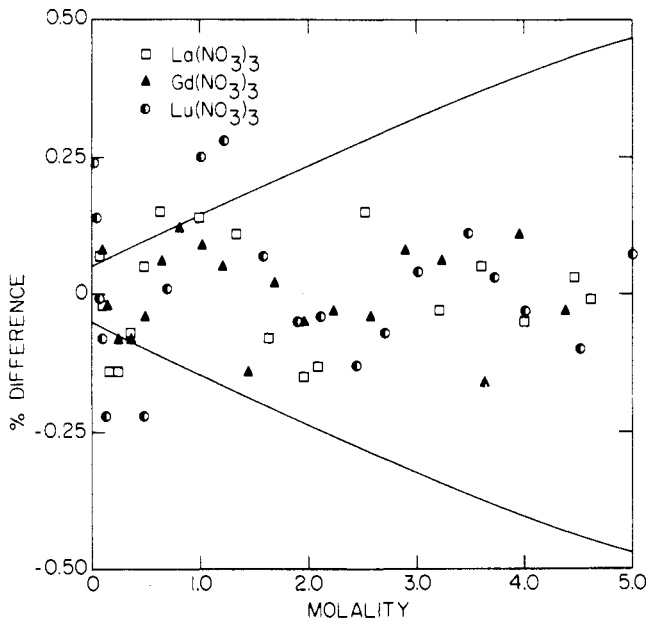


Figure 2. Percent differences between calculated and experimental viscosities. Solid curves represent total probable errors

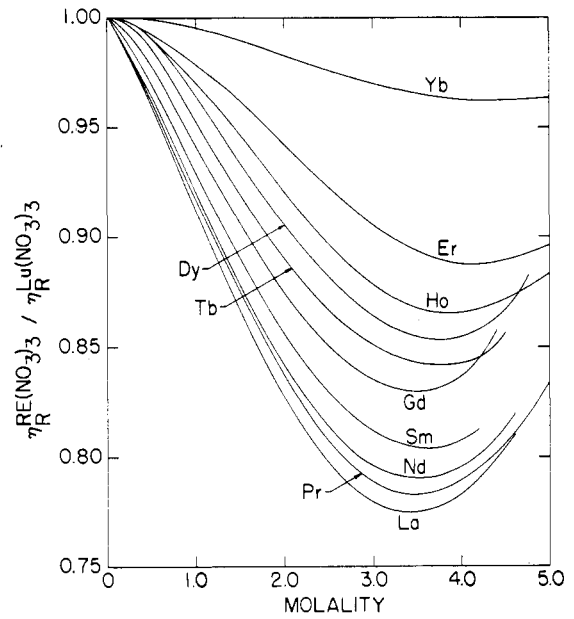


Figure 3. Ratios of aqueous rare earth nitrate viscosities to those of $\text{Lu}(\text{NO}_3)_3$ at 25°C

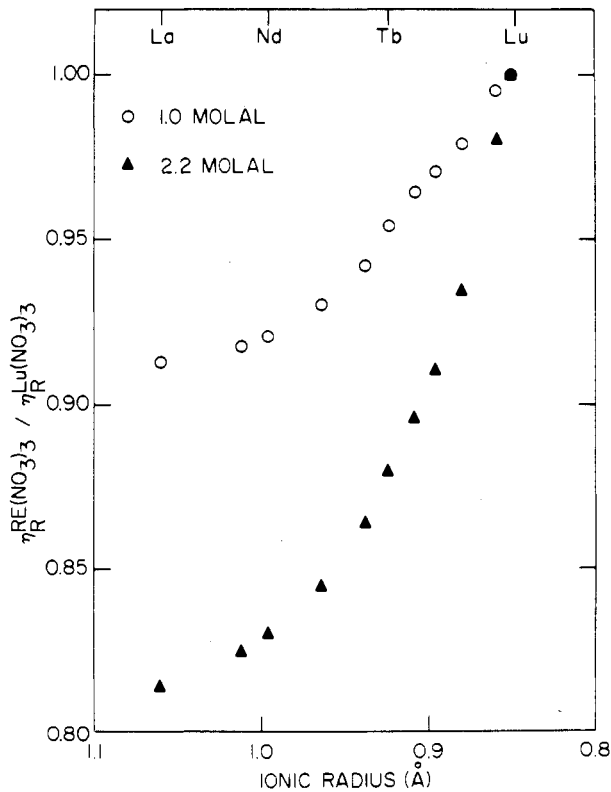


Figure 4. Ratio plots for rare earth nitrates as function of cation radius

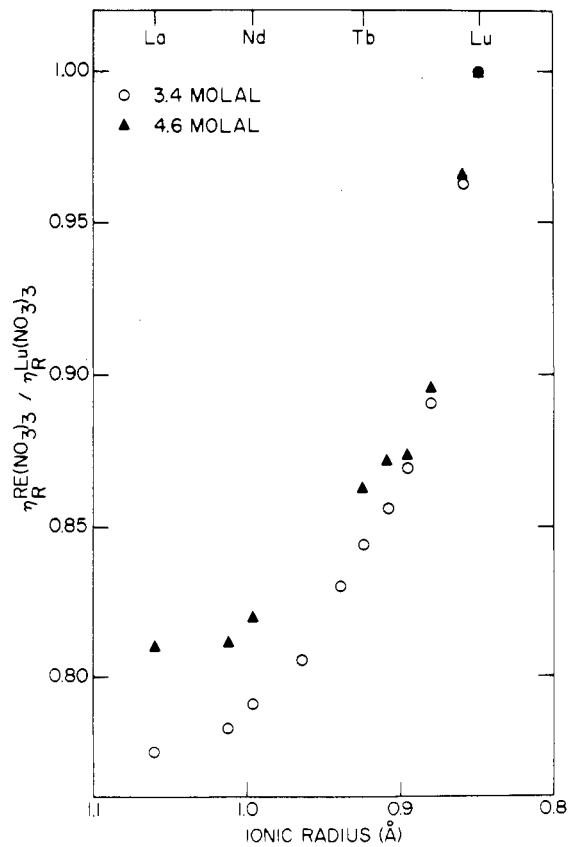


Figure 5. Ratio plots for rare earth nitrates as function of cation radius

the Jones-Dole equation applied up to 0.1*m* for the rare earth chlorides and perchlorates but has already broken down in the nitrates because of complexation at much lower concentrations. Consequently, the data of this research could not be used to evaluate significant Jones-Dole parameters for the nitrates.

At higher molalities the rare earth nitrate viscosities increase from La to Lu at constant molality (neglecting the possible crossings near saturation mentioned above). A high concentration modification in behavior is beginning to occur in the rare earth chlorides (13, 19) and becomes fully established in the perchlorates (18) by 3.5*m*. At these high concentrations, the rare earth perchlorate viscosity at constant molality rises from La to Nd, decreases to Tb, and then rises again to Lu. Related effects also appear in the electrical conductances of these salts (15, 16).

This behavior was attributed to a general increase in viscosity across the rare earth series owing to a net increase in the number of waters bound by the rare earth ion as the lanthanide contraction gives rise to an increase in the surface charge density on the ion. This increase in viscosity across the series is modified by a change in the inner sphere hydration number between Nd and Tb and gives rise to both the high concentration two-series behavior and the S shape at lower concentrations. This mechanism involves the retention of the complete inner sphere hydration sheath of the rare earth ions at all concentrations. The retention of the hydration sheath by the rare earth ions has recently been confirmed by X-ray diffraction studies of nearly saturated rare earth chloride solutions (6) and a nearly saturated rare earth perchlorate solution (7). That is, anions do not penetrate the inner hydration sphere of the rare earth ions in solutions of these stoichiometric salts.

The absence of the same two-series behavior in the nitrates is not very surprising since the nitrate ions probably penetrate the rare earth ion's inner hydration sphere and displace water. The release of this inner sphere

water into the system also qualitatively accounts for the fact that the viscosity of each rare earth nitrate is lower than that of the corresponding chloride and perchlorate. Since electrical conductance data give more direct information about changes in complexation across the rare earth series, the nitrate viscosities will be discussed in more detail when the conductances are being considered (9).

Acknowledgment

The rare earth oxides were purified by J. E. Powell's group at the Ames Laboratory by use of ion-exchange methods. The authors thank A. Habenschuss for valuable discussions concerning this work.

Literature Cited

- (1) Abrahamer, I., Marcus, Y., *Inorg. Chem.*, **6**, 2103 (1967).
- (2) Choppin, G. R., Henrie, D. E., Buijs, K., *ibid.*, **5**, 1743 (1966).
- (3) Choppin, G. R., Strazik, W. F., *ibid.*, **4**, 1250 (1965).
- (4) Knoeck, J., *Anal. Chem.*, **41**, 2069 (1969).
- (5) Marcus, Y., Abrahamer, I., *J. Inorg. Nucl. Chem.*, **22**, 141 (1961).
- (6) Martin, L. L., Spedding, F. H., *J. Chem. Phys.*, submitted for publication (1974).
- (7) Martin, L. L., Spedding, F. H., unpublished data.
- (8) Nelson, D. L., Irish, D. E., *J. Chem. Phys.*, **54**, 4479 (1971).
- (9) Rard, J. A., Spedding, F. H., *J. Phys. Chem.*, in press (1974).
- (10) Reuben, J., Fiat, D., *J. Chem. Phys.*, **51**, 4909 (1969).
- (11) Rumanova, I. M., Volidina, G. F., Belov, N. V., *Kristallografiya*, **9**, 624, 642 (1964); transl. in *Cryst.*, **9**, 545 (1965).
- (12) Spedding, F. H., Cullen, P. F., Habenschuss, A., *J. Phys. Chem.*, **78**, 1106 (1974).
- (13) Spedding, F. H., Pikal, M. J., *ibid.*, **70**, 2430 (1966).
- (14) Spedding, F. H., Pikal, M. J., Ayers, B. O., *ibid.*, p 2440.
- (15) Spedding, F. H., Rard, J. A., *ibid.*, **78**, 1435 (1974).
- (16) Spedding, F. H., Rard, J. A., Saeger, V. W., *J. Chem. Eng. Data*, **19** (4), 373 (1974).
- (17) Spedding, F. H., Shiers, L. E., Baker, J. L., Brown, M. A., Derer, J. L., Habenschuss, A., *J. Phys. Chem.*, submitted for publication (1974).
- (18) Spedding, F. H., Shiers, L. E., Rard, J. A., *J. Chem. Eng. Data*, **20** (1), 66 (1975).
- (19) Spedding, F. H., Witte, D., Shiers, L. E., Rard, J. A., *ibid.*, **19** (4), 369 (1974).
- (20) Templeton, D. H., Dauben, C. H., *J. Amer. Chem. Soc.*, **76**, 5237 (1954).

Received for review June 24, 1974. Accepted August 22, 1974.

Equilibrium-Phase Properties of Isopentane-Carbon Dioxide System

George J. Besserer¹ and Donald B. Robinson²

Department of Chemical Engineering, University of Alberta, Edmonton, Alta., Canada

Vapor and liquid equilibrium-phase compositions and refractive indices were determined for the isopentane-carbon dioxide system at 40.0°, 100.0°, 160.1°, and 220.1°F from the vapor pressure of isopentane to pressures in the critical region. The equilibrium ratios were calculated for each component at each temperature from the phase composition data. The equilibrium-phase densities were calculated from the measured phase composition and refractive index by use of the Lorentz-Lorenz molar refractivity relationship.

A systematic study of the literature pertaining to the phase behavior relationships of carbon dioxide-paraffin hydrocarbon binaries did not reveal any published data

¹Present address, Mon Max—H and G Services Ltd., Calgary, Alta., Canada.

²To whom correspondence should be addressed.

on the carbon dioxide-isopentane system. Data of this kind are useful for the evaluation of binary interaction coefficients required in equation of state or other generalized vapor-liquid equilibrium correlations and for the determination of the Henry's Law constant for carbon dioxide dissolved in isopentane. Accordingly, it was decided to carry out an experimental study of the system in the temperature range from 40° to 220°F.

Experimental Method

The experimental equipment and procedures were essentially the same as those described in earlier papers by Besserer and Robinson (1, 5). Measurements were made at each of four temperatures which were nominally 40°, 100°, 160°, and 220°F. At each temperature, measurements of the equilibrium-phase compositions and refractive indices were made at a series of pressures between the vapor pressure of isopentane and the vapor pressure